Nuclear Magnetic Resonance of H^1 and F^{19} Nuclei

William Grenard

December 14, 2015

Abstract

Continuous wave NMR techniques were used to determine the ratio of the magnetic moment of F^{19} to that of H^1 by measuring the resonant frequencies in Teflon and glycerin, respectively. The value of this ratio reported here is 0.94081 ± 0.00005 and is in agreement with that reported by Poss [1]. By recording the line width of water samples in the presence of Mn++ ions, the transverse relaxation time for deuteron is verified to increase with increased presence of paramagnetic ions. In addition, using pulsed NMR techniques, the transverse relaxation time for glycerin is determined and is reported here to be 2.1 ± 0.4ms.

1 Introduction

Nuclear magnetic resonance (NMR) is a very powerful tool which can be used to study the structure of atomic nuclei as well as the atomic structure of molecular compounds. Firstly, it can be used to precisely determine the magnetic moments of nuclei. In this experiment, the observation of NMR in glycerin and Teflon was used to precisely determine the ratio of the magnetic moments of the H^1 and F^{19} nuclei.

Moreover, NMR can provide insight about the local magnetic environment surrounding nuclei of various molecular compounds. In this experiment, the transverse relaxation time was measured for glycerin, providing information about the environment of the H^1 nuclei in this compound. In addition, observations on the NMR line width for several water samples containing various concentrations of the ion Mn++ allowed us to draw conclusions about the dependence of the magnetic environment on the presence of these ions in the sample.

2 Theory

2.1 The Undamped Bloch Equations

It is known that an atomic nucleus possesses a magnetic moment that is proportional to its angular momentum. Denoting the magnetic moment of a given nucleus by the vector operator $\boldsymbol{\mu}$, and its angular momentum by $\boldsymbol{L}$, this relationship is expressed as:

$$\boldsymbol{\mu} = \gamma \boldsymbol{L} \tag{1}$$

where the proportionality factor γ, is often called the gyromagnetic ratio.

If one resorts to a classical picture of the nucleus, this relationship has a nice intuitive motivation. In this picture, one may think of the nucleus as a tiny spinning electrically charged ball. This spinning has the effect of creating a small current loop. Because the current is proportional to the angular momentum of the spinning nucleus, and the magnetic moment of a current loop is proportional to the current, it is quite easy to understand why the magnetic moment of the nucleus should be proportional to its angular momentum.

Now, if the nucleus in question is placed in an external magnetic field $\boldsymbol{B_o}$, our knowledge of electromagnetism tells us that the magnetic moment will experience a torque given by

$$\boldsymbol{\tau} = \boldsymbol{\mu} \times \boldsymbol{B_o} \tag{2}$$

which causes the magnetic moment to precess about the magnetic field. Quantum mechanics dictates that there are only two allowed precession angles between the magnetic moment and the external field. One of these angles corresponds to the magnetic moment precessing about an axis aligned to the external field, and the other corresponds to the magnetic moment precessing about an axis antialigned to the external field.

If we consider placing a sample with many nuclei in a magnetic field, each of the nuclei precess either aligned or antialigned to the applied field. The energy difference between these two cases is quite small in comparison to thermal fluctuations at room temperature. As a result, the population of nuclei in each of the states follows the Boltzmann distribution in thermal equilibrium, with the majority of nuclei being in the state aligned with the field, as this is the state with the least energy. The result is a net magnetization of the material along the direction of the applied magnetic field.

Mathematically speaking, the change in magnetization due to the external magnetic field is expressed by the Bloch equations, which are easily determined

in terms of classical torque on the magnetic moments. Because the torque is equal to the time derivative of the angular momentum we can use Equations 1 and 2 to show that

$$\boldsymbol{\tau} = \frac{1}{\gamma}\frac{d\boldsymbol{\mu}}{dt} = \boldsymbol{\mu} \times \boldsymbol{B_o} \tag{3}$$

And therefore we have that

$$\frac{d\boldsymbol{\mu}}{dt} = \gamma\boldsymbol{\mu} \times \boldsymbol{B_o} \tag{4}$$

By noting that the magnetization of a unit volume of the sample is given by the sum of all the magnetic moments within the volume, if we denote the magnetization vector by $\mathbf{M}$, Equation 4 implies

$$\frac{d\mathbf{M}}{dt} = \gamma\mathbf{M} \times \boldsymbol{B_o} \tag{5}$$

This vector equation may be separated into three differential equations: one for M_x, M_y, and M_z. These are the undamped Bloch equations, and they describe the precessional motion of the magnetization in an idealized case.

As they are presented above, these equations are wildly inaccurate in describing the actual time evolution of the magnetization. This is, in a major part, because we have made two unphysical assumptions in their derivation: (1) that the only force effecting the motion of the magnetization is the applied magnetic field, and (2) that the magnetic field is constant throughout the entire sample of nuclei. In the next sections, well remove each of these assumptions and explore the resulting effects on the time evolution of the magnetization.

2.2 Dampening of the Bloch Equations

Imagine applying a constant magnetic field in the z-direction to a sample of nuclei. According to the undamped Bloch equations, the magnetization throughout the sample should simply precess about the applied field forever. However, the physical reality is that the magnetization eventually becomes strictly aligned along the z-direction.

A parallel may be drawn to the precession of a spinning top. According to idealized theory, one could devise situations where a top would precess infinitely. In reality, however, energy is lost through frictional forces, and eventually, the top falls over and ceases to precess.

In a similar manner, the magnetic energy of the nuclei the magnetic field is decreased by interactions with the surrounding lattice, causing the magnetization to align with the field over time. A fairly accurate model of this is dictated

by the assumption that the z component of the magnetization approaches its equilibrium value M_o at a rate proportional to its difference from equilibrium. This is expressed as

$$\frac{dM_z}{dt} = \frac{M_o - M_z}{T_1} \tag{6}$$

Here, T_1 is called the longitudinal relaxation time. It is a measure of how quickly the magnetization in the z direction reaches its equilibrium value after being placed in the magnetic field.

The same model can be used for the relaxation of the x and y components of the magnetization. Because the equilibrium values for these components are zero, the expressions equivalent to Equation 6, are simply

$$\frac{dM_x}{dt} = -\frac{M_x}{T_2} \tag{7}$$

$$\frac{dM_y}{dt} = -\frac{M_y}{T_2} \tag{8}$$

Here, T_2 is called the transverse relaxation time, and is a measure of how quickly the transverse components of the magnetization decay to zero. The main cause of this decay is due to inhomogeneities in the magnetic field at different areas of the sample. This is due to local fields within the atoms.

Differing fields cause the nuclear moments to precess at different frequencies throughout the sample. Over time, this causes a dephasing of the moments. Since the magnetization in a given volume is simply the sum of all of the magnetic moments within said volume, this dephasing eventually results in a net sum of zero magnetization in the x and y directions. Thus, T_2 is a measure of the dephasing time.

2.3 Resonance

The undamped Bloch equations along with the dampening conditions introduced in the previous section may be combined to form the three damped Bloch equations

$$\frac{dM_z}{dt} = \gamma(\mathbf{M} \times \boldsymbol{B_o})_z + \frac{M_o - M_z}{T_1} \tag{9}$$

$$\frac{dM_x}{dt} = \gamma(\mathbf{M} \times \boldsymbol{B_o})_x - \frac{M_x}{T_2} \tag{10}$$

$$\frac{dM_y}{dt} = \gamma(\mathbf{M} \times \boldsymbol{B_o})_y - \frac{M_y}{T_2} \tag{11}$$

This system of differential equations, when solved, shows that the transverse components of the magnetization behave like a damped harmonic oscillator in two dimensions, with a resonant frequency given by

$$\omega = \gamma B_o \tag{12}$$

The specifics of this calculation is explained by Kittel [2].

The frequency ω is precisely the precessional frequency of the magnetic moments, and the parallel drawn between this system and a damped harmonic oscillator suggests that if the system is driven with a magnetic field of frequency ω in the transverse direction, resonance will occur.

The exact frequency at which this resonance condition is met is dependent upon the magnetic field, as well as the gyromagnetic ratio of the nuclei involved. Because of this, valuable information may be gleaned about the fields local to the nuclei, as well as the magnetic moments of the nuclei.

2.4 Observing Resonance: Pulsed and CW NMR

It is quite simple to detect the frequency at which resonance occurs by placing a sample of nuclei in a constant magnetic field oriented in a direction we will label as the z direction, and wrapping the sample with a coil of wire connected to some type of detection system. Then, one only needs to apply an oscillating magnetic field in a direction perpendicular to the z direction.

The frequency of this latter signal can be adjusted slowly, and when the resonance condition is met the magnetization of the sample will precess, causing a time varying magnetic flux, which will induce a detectable voltage in the coil. By searching for the driving frequency which produces a maximum induced voltage, the resonant frequency may be found.

With this method it can be difficult to determine exactly when the induced voltage reaches its maximum, so a slight modification to this method is in order. Instead of varying the driving frequency, one can keep this value constant and instead vary the strength of the external magnetic field in which the sample is placed.

By oscillating the magnitude of the external field around the value of the field at which resonance occurs for a given driving frequency, one can amplitude modulate the voltage signal that is produced on and near resonance. Each time the magnitude of the field passes the resonant value, there will be a peak in the amplitude of the received signal.

By employing the use of a bandpass filter, the amplitude of the voltage signal can be picked out and plotted against the magnetic field. The result

is a peak in the signal at the magnetic field corresponding to resonance. The plot is what is known as an absorption curve, and the location of the peak can be used to easily determine the resonant frequency.

An example of an absorption curve is shown in Figure 1(a), and a dispersion curve–simply an alternate mode of the same graph–is shown in Figure 1(b). In this image, there are two peaks simply because the magnetic field was swept twice over the resonance value, and a peak is visible for each of these passes.

The detection method described above is known as continuous wave (CW) NMR for the reason that the transverse oscillating field is applied constantly throughout the experiment. Another method, known as pulsed NMR can be used to determine more information about the relaxation times T_1 and T_2 once the resonance frequency is found by means of CW NMR.

In a pulsed NMR experiment the transverse field is applied in a short burst to deflect the magnetization from its thermal equilibrium in the z direction into the x-y plane. Initially, after this is done the magnetization will precess about the z direction, meaning that the magnetic moments are all in phase and precessing together. The resulting voltage signal can be recorded after this initial pulse. However, some time after the pulse is given, the individual moments will become out of phase due to inhomogeneities in the magnetic field, as described in Section 2.2. Because of this, the amplitude of the induced voltage will slowly decay to zero.

Once this dephasing has occurred, another pulse lasting twice the length of the first, can be applied to the sample to kick the magnetic moments by a full 180°. This has the effect of reversing the dephasing process because it essentially reverses the order in which each moment precesses. Thus, the moments slowly return back to the way they were originally after the first pulse. That is, they become in phase again, and once again a voltage is induced and can be detected. This is known as the spin echo effect.

It is not difficult to see that the dephasing time T_2 is related to the time it takes for the voltage amplitude to decay to zero. In addition, the longitudinal relaxation time T_1 can be determined by lengthening the time between the two pulses. Eventually, the second pulse will come after the magnetization has relaxed back to its thermal equilibrium in the z direction. If this occurs, a second pulse will not produce a spin echo effect.

Finally, it is important to note that there are some connections between these relaxation times and continuous wave NMR. Firstly, in an absorption trace found by continuous wave NMR techniques, field inhomogeneities can effect the trace in a similar way that it effects T_2. For example, there is a possibility of observing a string of decaying oscillations immediately after the absorption peak. This can occur because immediately after the external field

is swept through the resonant value, the magnetization may spend additional time precessing before settling back down to its non resonant equilibrium value. A larger amount of these oscillations indicates that the magnetic field throughout the sample is fairly homogeneous, because the magnetic moments are able to stay in phase with each other long enough to observe the decaying signal.

In addition, the absorption curve from a continuous wave experiment is theoretically the Fourier transform of the decay envelope of a pulsed NMR experiment. This relationship causes the full width at half maximum of the absorption curve to be equal to $1/T_2$.

3 Apparatus

For the first part of the experiment, a continuous wave NMR technique is used. This consists of continuously applying a driving magnetic field at the resonant frequency and observing the response of various samples. Samples used include glycerin and water with various levels of Mn++ added.

The samples themselves, contained in small test tubes, are inserted into a box called the NMR head, which is itself placed between the poles of a permanent magnet. In addition to holding the sample within the external magnetic field the NMR head has three main functions.

The first function is to transmit the signal which will induce resonance in the sample. This is done with a coil of wire that produces an oscillating magnetic field perpendicular to the field of the permanent magnet when supplied with a signal from the NMR black box. This box provides the ability to apply transverse fields oscillating at a given frequency. A frequency counter is used to measure the frequency being applied at any given time.

The second function of the NMR head is to receive the voltage induced by the precession of the magnetization at resonance. This is done, as explained in the previous section, by a coil of wire wrapped around the housing of the test tube. The voltage induced in this coil is sent back out to the NMR black box where it is amplified and sent to a detection setup. The phase between the transmitted and received signal can be altered by turning a small copper plate within the NMR head, effecting the appearance of the received signal.

Finally, there are a pair of wire coils on the top and bottom of the NMR head. These coils are sent an alternating signal of 60Hz, producing an oscillating magnetic field parallel to the field applied by the permanent magnet. This has the effect of modulating the external magnetic field about the resonant value.

Note that for glycerin and water, the resonant frequencies are 16MHz,

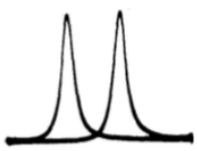

(a) Absorption

(b) Dispersion

Figure 1: Resonance Curves. *Images from Yuan and Wu* [3].

many orders of magnitude larger than the modulation frequency of 60Hz. The result, then, of modulating the external field around resonance is to produce a 16MHz voltage signal from the receiver coils that is modulated at 60Hz. By running the signal through a bandpass filter, the carrier frequency is removed, leaving only the modulation envelope. After amplification, the signal is displayed on an oscilloscope in x-y mode, using the amplitude of the signal from the receiver coils on the y axis, and the external magnetic field on the x axis.

The result of this setup is to produce scope traces similar to those shown in Figure 1. The differing shapes, known as the absorption and dispersion modes, are simply due to a differing phase between the transverse oscillating signal and the signal induced by the precessing magnetization. Both of these curves can be achieved by rotating the copper plate in the NMR head.

The peaks seen in the images occur when the external magnetic field passes the resonant value. By adjusting the transverse frequency with the NMR black box, the position of the peaks can be positioned symmetrically around the center of the scope trace, indicating for that frequency, the external magnetic field is oscillating symmetrically about the resonant value. Therefore, the frequency read on the frequency counter is precisely the resonant frequency.

For observing the line width of the water samples, a lock in trace was produced, rather than simply viewing the signal on the oscilloscope. This was done to drastically increase the signal to noise ratio for a more accurate determination of line widths.

Finally, in the pulsed NMR portion of the experiment, the NMR head was replaced with another box called the pulsed NMR head. This box is designed to hold the samples for the pulsed NMR experiment, to send the signal pulses into the sample, and to receive the resulting induced voltage, very similar to the NMR head.

The main difference in the setup for this part of the experiment is that a pulse generator is used to produce two pulses of a transverse oscillating magnetic field in the sample, rather than applying this field continuously. The pulse generator allowed for varying the length of the pulses, as well as the time

between them.

4 Procedure

4.1 Continuous Wave NMR

First, the magnetic field of the permanent magnet in which the samples were placed was measured. This was done by inserting a glycerin sample into the NMR head and locating the absorption curve on the oscilloscope. Once the curve was located, the position of the NMR head was adjusted to the place where the most "wiggles" were visible. Then, the frequency at which the curve was centered on the scope trace was recorded several different times under identical conditions.

The resonance observed for glycerin corresponds to the magnetic moment of H^1. Thus, using the known value of the gyromagnetic ratio of the proton, the external field was calculated via Equation 12.

Using this information, the axis on the trace were calibrated by noting that the ratio between the resonant frequency and the external field is a constant. In fact, from Equation 12, one can see that $\frac{\omega}{B_o} = \gamma$.

To make use of this fact, the frequency was altered so that the peak of the absorption curve sat one division to the right of the center. The ratio of the magnetic field at this point on the scope trace to the new frequency value must be the same as the ratio of the magnetic field at the center to the first resonant frequency measured. Using this fact, the axis was calibrated to be 1G/div.

Next, in order to measure the ratio of the magnetic moments F^{19} and H^1, a Teflon rod was inserted into the NMR head. The resonant frequency of Teflon is due to F^{19}. Thus, by writing Equation 12 out for both the H^1 and F^{19} nuclei, and then dividing the equations, it is found that the ratio of the magnetic moments we seek is given by

$$\frac{\gamma_{F^{19}}}{\gamma_{H^1}} = \frac{f_{F^{19}}}{f_{H^1}} \tag{13}$$

That is, the ratio of the magnetic moments is equal to the ratio of the resonant frequencies, assuming the field of the permanent magnet stays constant throughout the experiment.

Using the same method that was used for measuring the resonant frequency for glycerin, the resonant frequency of the Teflon was recorded and used to calculate the desired ratio.

Finally, to observe the effect of paramagnetic ions on relaxation times, lock in traces of the absorption curves for water containing 0.033M, 0.1M, 0.33M, 1M, and 3.3M Mn++ ions were obtained. The line widths of the curves for each sample were compared.

4.2 Pulsed NMR

Next, the pulse generator was used to send frequency pulses into a glycerin sample housed in the pulsed NMR head. After much experimenting with the length of the pulses, and the width between them a spin echo effect was observed on a LabView time average of the signal coming from the pulsed NMR head.

In order to achieve this, the second pulse was made to be twice as long as the first. This has the effect of producing a 90° and 180° flip of the magnetic moments, once the length of the first pulse is calibrated properly. The proper length to produce a 90° kick in the moments was found simply by altering the length until the best"ringing" was observed in the LabView plot. Clear ringing is a sign that the moments have been displaced a significant angle outward from the z direction, and the best signal should occur when the moments are angled at approximately 90° from the external field.

Once the spin echo was successfully observed, the time between pulses was increased and the spin echo was observed again. This process of lengthening the width between pulses was repeated many times until the amplitude of the spin echo was reduced to zero.

5 Results and Analysis

5.1 Magnetic Field and Ratio of Moments

The magnetic field of the permanent magnet used in this experiment was successfully measured from the absorption curve of glycerin. A typical glycerin absorption curve is shown in Figure 2.

In this figure, there are two clear peaks in the amplitude of the voltage signal induced as the external field was swept past the resonant value. At the base of the rightmost peak, ringing is clearly visible in the signal, indicating a fair level of homogeneity in the magnetic field, as explained in Section 2.

The driving frequency which produced these symmetric peaks, namely the resonant frequency of H^1 was recorded several times in a row under identical conditions. In order to ensure that the magnetic field at the location

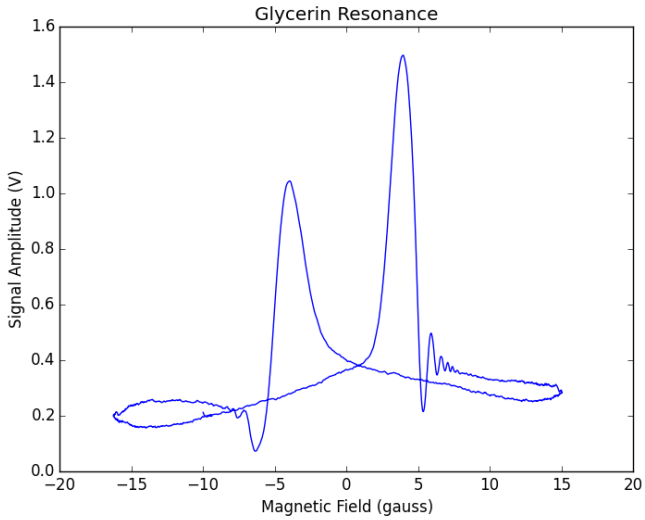

Figure 2: Absorption curve for glycerin.

of the NMR head would remain fairly constant throughout the experiment, this datataking process was repeated on two different days, and the results compared. The results of these measurements are shown in Table 1.

Table 1: H^1 Resonance Frequencies

Day 1 Resonant Frequency (MHz)	Day 2 Resonant Frequency (MHz)
16.04089	16.04150
16.04116	16.04052
16.04061	16.04172
16.04120	16.04161

By averaging these data points and taking the uncertainty to be equal to 1 standard deviation, the resonant frequency on day 1 and day 2 was found to be:

$$(f_{H^1})_1 = 16.0413 \pm 0.0005\,\text{MHz} \tag{14}$$

$$(f_{H^1})_2 = 16.0410 \pm 0.0003\,\text{MHz} \tag{15}$$

Then, by use of Equation 12, the magnetic field value was calculated for each

day. The uncertainties presented are those propagated through Equation 12.

$$B_1 = 3.7675 \pm 0.0001 \text{ kG} \tag{16}$$

$$B_2 = 3.76748 \pm 0.00007 \text{ kG} \tag{17}$$

These values clearly agree very well, and thus it was assumed throughout the rest of the experiment that the magnetic field could be safely taken as constant.

For the following calculation of the magnetic moment of F^{19}, the value $(f_{H^1})_2$ is used, because the data for the F^{19} nuclei was taken on the same day this frequency was measured. Henceforth, this quantity will simply be denoted f_{H^1}.

Next, both the absorption and dispersion curves for the Teflon sample are shown in Figures 3 and 4, respectively. Note that the peaks for this sample are not separated from each other as the peaks in the glycerin absorption curve. This is simply due to a different phase used in the display of this plot relative to the other, and is nothing special about Teflon.

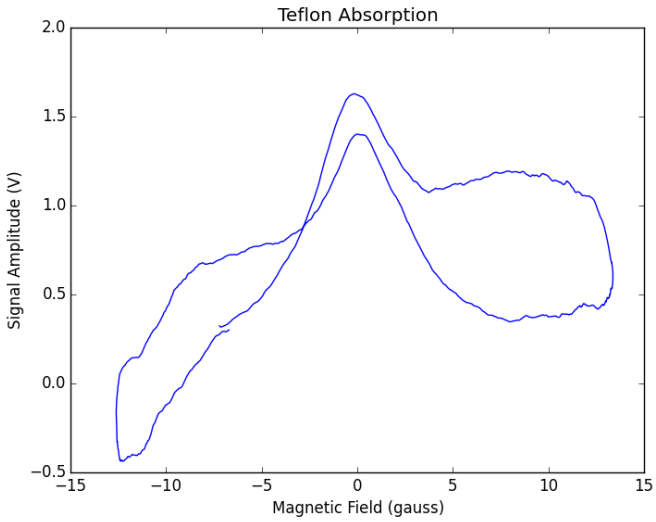

Figure 3: Absorption curve for Teflon.

Just as was done with the glycerin sample, the resonant frequency for F^{19} was determined by repeatedly centering the peaks and recording the corresponding driving frequency. The results are shown in Table 2.

Again, the average of these values with 1 standard deviation uncertainty is:

$$f_{F^{19}} = 15.0916 \pm 0.0007 \text{MHz} \tag{18}$$

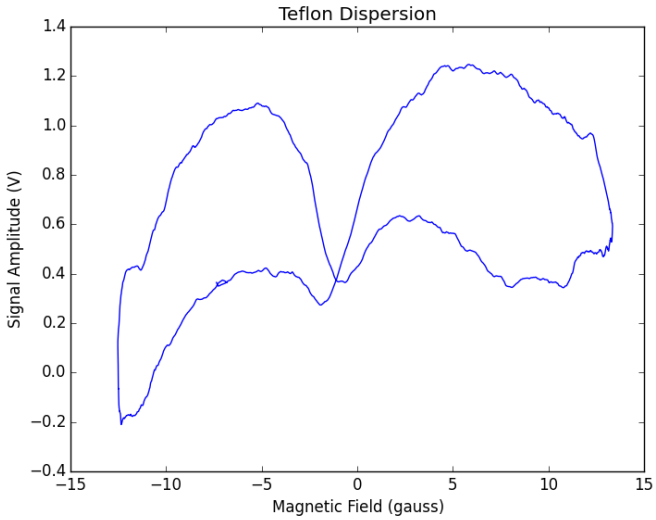

Figure 4: Dispersion curve for Teflon.

Table 2: F^{19} Resonance Frequencies

Resonant Frequency (MHz)
15.09157
15.09232
15.09197
15.09040

Next, after employing the use of Equation 13, and propagating through it the uncertainties in f_{H^1} and $f_{F^{19}}$ it is found that

$$\frac{\mu_{F19}}{\mu_{H1}} = 0.94081 \pm 0.00005 \tag{19}$$

This comfortably falls within 1 standard deviation of the accepted value of 0.94077 reported by Poss [1].

5.2 Line Width for H_2O with Mn++

A clear dependence was found between the line width of the NMR signal for deuteron and the molarity of paramagnetic ions Mn++ present in the sample. The lock in traces were taken for water with 0.033M, 0.1M, 0.33M, 1.0M, and 3.3M Mn++ ions mixed in.

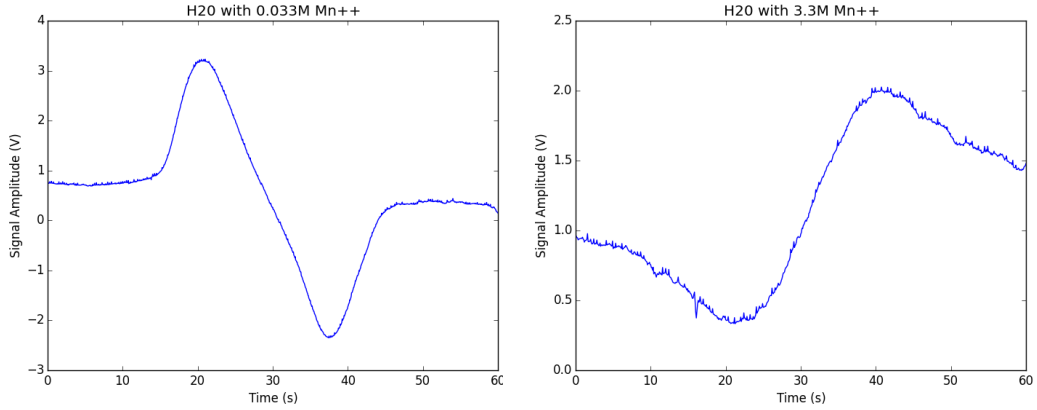

(a) 0.033M Mn++ (b) 3.3M Mn++

Figure 5: Lock in traces of dispersion curves for water containing Mn++.

Each of the traces is qualitatively the same, save that the line width visibly increases as the molarity of Mn++ in the sample increases. Below in Figure 5 the lock in traces for water with 0.033M and 3.3M Mn++ are shown for comparison.

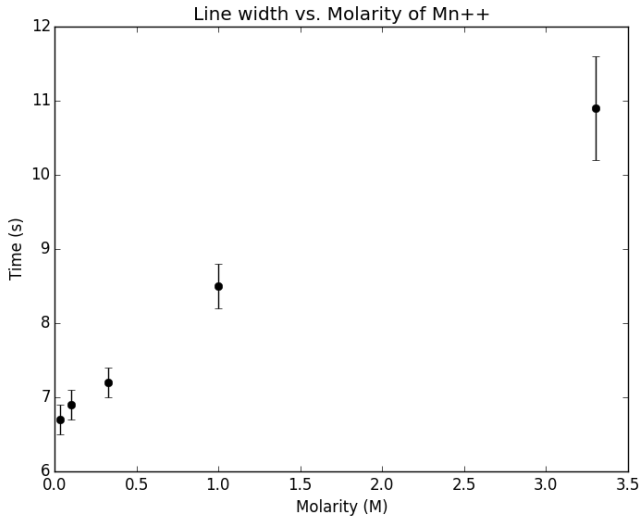

Figure 6: Line width versus molarity of Mn++

The time referred to on the horizontal axes of these graphs is the time taken to sweep the magnitude of the external magnetic field. Unfortunately,

insufficient data prevented the scaling of the horizontal axis to units of gauss. This is because the magnitude of the magnetic field sweep generated in order to take the lock in data is unknown. I am forced, therefore, to leave the horizontal axis in units of time.

The consequence of this is that the exact line width in Gauss is not determinable. However, because the time is proportional to the magnetic field, the line width broadening pattern which is exhibited in the data is completely valid. Figure 6 shows this pattern more clearly, by displaying the line width in seconds (which is proportional to the line width in gauss) against the molarity of Mn++ present in the sample.

The uncertainties reported in this figure were estimated from upper and lower bounds of the line widths as determined from the lock in traces. The uncertainty increased sharply for the line width of the 3.3M sample. This is due to increased noise in the lock in signal, which created a larger spread of possible line widths.

Though the data does not fit well to a linear regression, there is still a clear trend of increasing line width as the concentration of Mn++ is increased up to 3.3M. As Mn++ is a paramagnetic ion, this trend is expected. Increased levels of Mn++ in the sample create larger inhomogeneities in the local magnetic field within the sample. This is expected to decrease the dephasing time of the magnetic moments, which in turn would increase the line width.

5.3 The Spin Echo Effect in Glycerin

The spin echo effect for a glycerin sample was successfully obtained. The clearest example able to be found was with a 10ms spacing between pulses and is shown in Figure 7.

The growth rate of the spin echo "wiggles" was used to calculate the dephasing time T_2, by fitting the growth to an exponential. This fit is shown in Figure 8.

The data was taken for this fit by recording the height of successive peaks of the spin echo shown in Figure 7 as it grew from nearly zero to its maximum value. Uncertainties in individual points were estimated by the range of possible peak values as read from the figure.

The exponential fit of $y = Ae^{Bx} + C$ gives a value of 0.5 ± 0.1 ms^{-1} for the time constant B. Thus, it is found that:

$$T_2 = \frac{1}{B} = 2.1 \pm 0.4\text{ms} \tag{20}$$

Note that there are deviations from the fit and the data which are larger

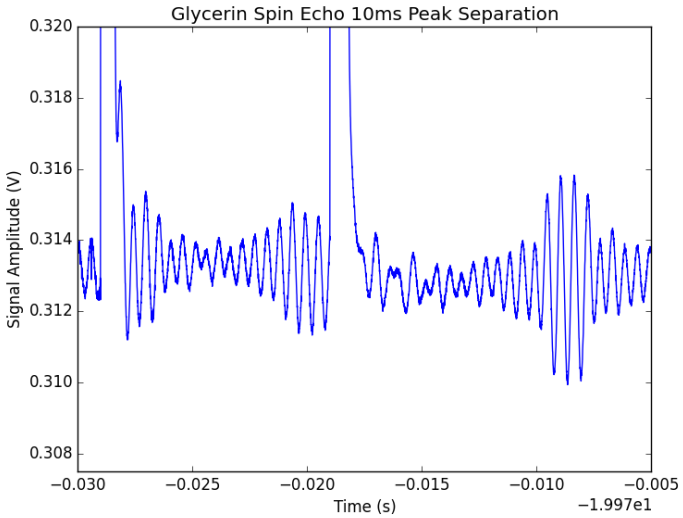

Figure 7: The spin echo effect in glycerin.

than the uncertainties reported. It is believed this is because the spin echo effect observed in Figure 7 was not ideal. It is clear that the oscillations never decay completely to zero throughout the plot. A cleaner spin echo effect would present an amplitude decay to very near zero before the occurrence of the echo. It is believed that if a better trace can be obtained, the data will better fit the exponential, and a more accurate determination of T_2 may be found.

Unfortunately, the data to be used to determine T_1 is unusable, and an estimate of this time is not presented here. Though the LabView traces of the data in the lab seemed to show the spin echo amplitude decreasing, further analysis of the data showed that this was not the case. Data was taken for spacing between the pulses of up to 25ms, and the spin echo effect is still present. Though the signal is not as clean as the one presented in Figure 7, the amplitude of the spin echo seems to be roughly the same.

It is thus concluded that T_1 is appreciably larger than 25ms, but no more information beyond this can be gleaned.

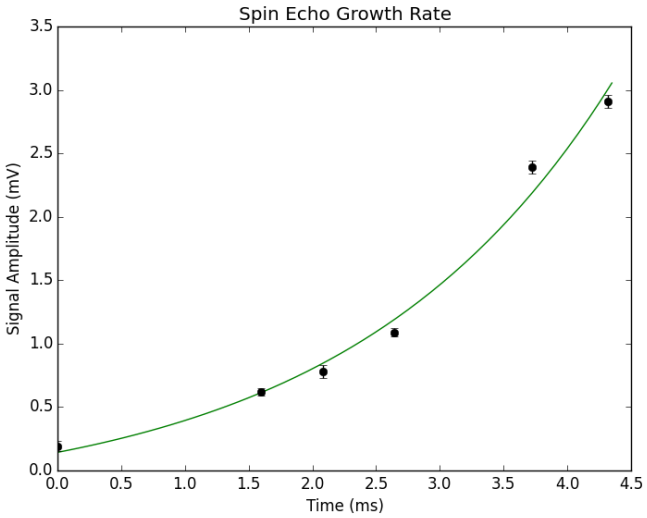

Figure 8: Growth Rate of Spin Echo in Glycerin.

References

[1] H. L. Poss, Phys. Rev. **75**, 600 (1949).

[2] Charles Kittel. *Introduction to Solid State Physics*. ed 8. John Wiley and Sons. 2005.

[3] L. Yuan and C.S. Wu Academic Press. Vol. 5, 104-123 (1963).